
ControlThinker: Unveiling Latent Semantics for Controllable Image Generation through Visual Reasoning

Feng Han^{1,2*} Yang Jiao^{1,2*} Shaoxiang Chen³ Junhao Xu^{1,2}
Jingjing Chen^{1,2} Yu-Gang Jiang^{1,2}

¹ Shanghai Key Lab of Intell. Info. Processing, School of CS, Fudan University

² Shanghai Collaborative Innovation Center on Intelligent Visual Computing

³ MiniMax

Abstract

The field of controllable image generation has seen significant advancements, with various architectures improving generation layout consistency with control signals. However, contemporary methods still face challenges in bridging the semantic gap between input text prompts with sparse semantics and the target images, often over-relying on low-level control signals to infer regional details. To address this challenge, we propose ControlThinker, a novel framework that employs a "comprehend-then-generate" paradigm. Firstly, by incentivizing the visual reasoning capability of a MLLM, latent semantics from control images are mined to enrich text prompts. This enriched semantic understanding then seamlessly aids in image generation without the need for additional complex modifications. To further tackle the uncertainty arising from the ambiguity of control images, we encourage broader exploration of reasoning trajectories and select the optimal one using a metric-based output reward model (ORM). Extensive experimental results demonstrate that ControlThinker effectively mitigates the semantic gap between raw text prompts and target images, resulting in improved visual quality and semantic consistency across a wide range of benchmarks. The code and models are available at <https://github.com/Maplebb/ControlThinker>

1 Introduction

In recent years, significant advancements [25, 28, 13, 2, 11] have been made in text-to-image generation, marked by enhanced comprehension of diverse textual prompts and improved aesthetic refinement in synthesized images. To achieve finer-grained control over image details, another line of research [33, 15, 18, 24] incorporates images depicting low-level scene properties as conditional inputs. The prevailing paradigm in this field builds upon pre-trained text-to-image foundation models, augmenting them with specialized modules to enhance visual controllability [29]. Within this domain, two major research strands are commonly explored. The first, which has been a longstanding focus, emphasizes diffusion-based architectures to enhance the layout accuracy of generated images. More recently, a second strand has emerged, employing auto-regressive generation architectures and concentrating on adapting visual controls to these models.

Despite considerable advancements, current methods largely neglect the substantial semantic gap between text prompts and target images, constraining the full potential of pre-trained text-to-image

*Equal contributions.

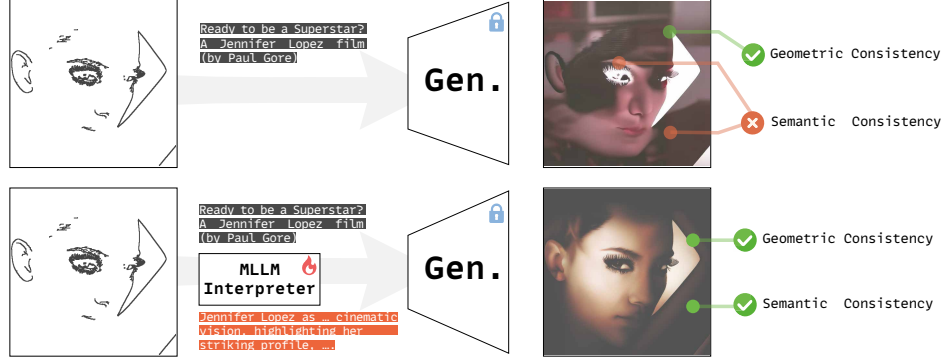


Figure 1: Comparison between our ControlThinker and previous works. Unlike previous approaches that struggle to address the semantic gap between input text prompts and target images, ControlThinker introduces an MLLM as a semantic interpreter to bridge this gap. By leveraging the MLLM’s reasoning capabilities, our framework effectively extracts and understands the latent semantics embedded in control images, thereby enabling the generator to achieve both geometric alignment and semantic coherence in the synthesized outputs.

generators. As shown in Fig. 1, the ambiguity of input text prompts¹ fails to provide semantically dense guidance for pixel-wise synthesis. This compels the model to reconstruct high-fidelity regional semantics solely from low-level control signals (e.g., depth/edge maps), thereby confronting a substantial leap in semantics. Such a requirement fundamentally deviates from the pre-trained text-to-image foundation models, which primarily establish mappings between linguistic concepts and the visual world. As a consequence, even the prevalent approaches struggle to generate semantically coherent regions with plausible visual rationales [18, 16]. As illustrated in Fig. 1, ControlAR [18] demonstrates limited semantic comprehension of the textual prompt “Jennifer Lopez”, relying primarily on the canny edge map to reconstruct regional details. Consequently, while the generated image maintains geometric consistency with the control signals, its semantic coherence catastrophically collapses.

To bridge this substantial semantic gap, we identify Multimodal Large Language Models (MLLMs) as a promising solution. Compared with text-to-image generation models, MLLMs [26, 6, 27] excel at parsing dense semantics and performing logical reasoning based on fundamental visual perceptions [3, 31, 32]. By introducing the MLLM as a sophisticated interpreter to uncover the latent semantics embedded in control images, the text-to-image generator can overcome the limitations of sparse semantic guidance, thereby enhancing generation quality. However, adapting an MLLM to the realm of controllable image generation is a non-trivial task. Unlike natural images, which are rich in color, texture, and contextual cues, control images (e.g., depth/edge maps) are structurally sparse, presenting significant challenges for semantic extraction [10]. This discrepancy between control signals and natural images further complicates the faithful generation of the target image.

Building on the above analysis, in this paper, we propose **ControlThinker**, a novel framework that enhances controllable image generation through improved visual reasoning. As shown in Fig. 1, our ControlThinker employs a “comprehend-then-generate” paradigm to effectively mine the latent semantics of control images. Specifically, rather than directly feeding the control image and text prompt into the image generator, we first leverage the modern MLLM, Qwen2.5-VL-7B [1], as an interpreter to explore the latent semantics in the control image, guided by the interaction with the input text prompt. However, in practice, we observe that prompting our MLLM for zero-shot comprehension fails to effectively mine latent semantics, as the model tends to be distracted by the dominant dark background or the unique styles of control images. To incentivize the visual reasoning capability in MLLM for comprehending control images, we curate a small-scale visual reasoning dataset specifically for control images and fine-tune the MLLM using both supervised (SFT) and reinforcement (RFT) techniques. After training, the MLLM can generate insightful chains of thought and produce enriched text prompts with dense semantics. Afterward, such enriched text prompts, together with the control image, are fed into the generator to synthesize the target image. Despite not tuning the generator, overall performance improves significantly, demonstrating that our ControlThinker effectively unlocks the potential of pre-trained text-to-image models. Additionally, while

¹This is an inherent limitation of text prompts in existing controllable image generation datasets, as evidenced by the statistics presented in Fig. 6.

the enriched text prompts exhibit significantly increased semantic density, they are still influenced by the uncertainty stemming from the inherent lack of detail in control images. To address this, we further expand the exploration of visual reasoning by sampling multiple reasoning trajectories from the MLLM and selecting the optimal one using a metric-based output reward model (ORM).

In summary, our contributions are three-folds: (1) We propose ControlThinker, a novel “comprehend-then-generate” framework that introduces MLLM as a wise semantic interpreter to mine latent semantics from control images. (2) To incentivize the visual reasoning capabilities toward control images, we fine-tune the MLLM using a combination of supervised (SFT) and reinforcement learning (RFT) strategies. Additionally, we address visual reasoning uncertainty with a metric-based ORM to further boost performance. (3) Extensive experiments demonstrate that ControlThinker significantly improves performance across multiple control types, achieving superior visual quality and semantic consistency without modifying the underlying image generators, confirming the effectiveness of our approach.

2 Related Work

2.1 Controllable Image Generation

Traditional text-to-image approaches [23, 8, 4] relying solely on textual prompts often fall short in satisfying users’ intentions of fine-grained generation. To enable precise control over pre-trained text-to-image diffusion models, additional visual control signals including Canny edges, HED boundaries, depth maps, and segmentation masks have been introduced as generation conditions. For instance, ControlNet [33] integrates these visual conditions through an auxiliary parallel branch created by duplicating the pre-trained model. However, this extra module notably increases computational cost overhead. In contrast, T2I-Adapter [22] offers a more efficient alternative with lightweight adapters, but sacrifices encoding capabilities for control images. More recently, ControlNet++ [15] addresses these limitations through a novel training paradigm, employing pixel-level cycle-consistency loss and efficient reward fine-tuning strategies to achieve more precise conditional control. Meanwhile, researchers have begun exploring multi-condition control [35, 9, 24] and instance-level control generation [30, 36]. Recently, ControlAR [18] explores efficient controllable image generation for the autoregressive image generation model and designs a control information encoding module that operates directly on input tokens. Nevertheless, current methods predominantly concentrate on improving the model’s capability to process textual and visual control signals, largely overlooking the intrinsic structural information inherent in control images. This structural information holds substantial potential for enriching the expressiveness of input textual prompts, thereby enhancing image generation quality from the very input stage.

2.2 Multimodal reasoning in image generation

The emergence of multimodal large language models (MLLMs) [1, 14] with advanced reasoning capabilities has inspired research on improving image generation quality through multimodal reasoning. For example, PARM++ [7] employs a fine-tuned reward model at test-time to select generation paths aligned with text inputs, enhancing text-image coherence but unsuitable for autoregressive VQ-VAE models. GoT [5] uses bounding boxes to plan object layouts, supporting precise image generation and editing. ImageGen-CoT [19] utilizes iterative prompt refinement for semantic alignment. However, in controllable generation tasks, control images inherently contain richer layout details than bounding boxes, making intermediate bounding boxes unnecessary. Effective multimodal reasoning thus requires analyzing these detailed layouts to enrich textual prompts with additional high-level semantics and low-level visual details, providing stronger control signals—an aspect ImageGen-CoT overlooks due to its semantic-centric approach.

3 Method

3.1 Preliminary: Basic Formulation of Controllable Image Generation

Controllable image generation aims to synthesize images that align with both the spatial layout defined by control images and the semantics conveyed by text prompts. Formally, taking a text

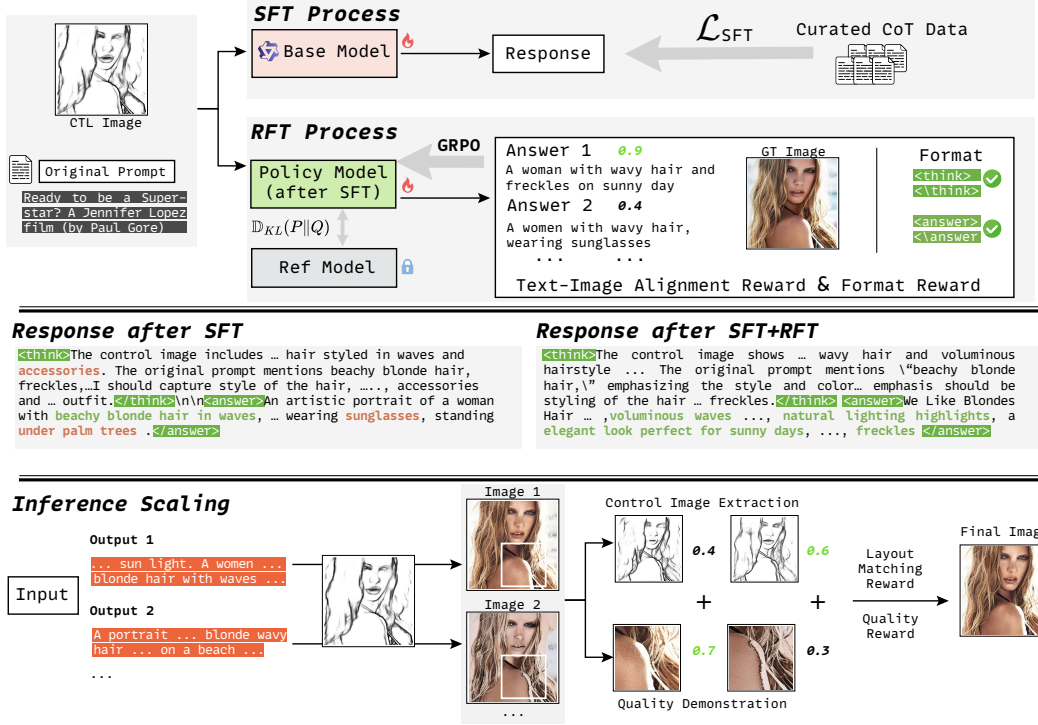


Figure 2: The SFT and RFT two stage training paradigm and Inference Scaling method of our ControlThinker.

prompt P_{orig} and a control image $I_{control}$ (e.g, depth/edge maps, segmentation masks) as input, the controllable image generation aims at generating a target image I_{target} as formulated below:

$$I_{target} = G(P_{orig}, I_{control}) \quad (1)$$

where G is the generation model. However, since P_{orig} typically conveys only coarse or underspecified semantics, it offers limited guidance for region-level synthesis. Consequently, the generation process tends to over-rely on $I_{control}$ to infer fine-grained semantic details of I_{target} , often resulting in semantics distortions in localized areas as discussed in Sec.1.

3.2 ControlThinker: Generation Driven by Enhanced Visual Reasoning

Our framework consists of three primary components that work in sequence to enhance visual reasoning capabilities. First, we curate a high-quality dataset comprises both chain-of-thought reasoning on control image and the original prompt, and the enhanced prompt with rich semantics. Besides, as illustrated in Fig. 2, we introduce a two-phase training strategy and inference scaling techniques for our ControlThinker. Specifically, our training strategy comprises supervised fine-tuning (SFT) on the curated chain-of-thought dataset to establish fundamental reasoning capabilities, followed by reinforcement fine-tuning (RFT), during which the policy model generates multiple reasoning trajectories. These trajectories are assessed with verifiable rewards and optimized through Group Preference Optimization (GRPO). Moreover, our inference scaling techniques effectively mitigate uncertainty in visual reasoning by selecting optimal outputs based on image quality and layout consistency. Collectively, these methodologies constitute a novel "comprehend-then-generate" paradigm, effectively bridging the semantic gap between sparse textual prompts and controllable images, significantly enhancing image generation quality without necessitating alterations to generator.

3.2.1 Data Curation

To enable effective visual reasoning from control images, we curate a specialized dataset that encourages the MLLM to generate enhanced prompts using powerful GPT-4o. Specifically, we prompt GPT-4o to analyze control images, identifying layout structures present in the control signal.

		Original Prompt	Zero Shot	After SFT	After SFT+RFT
GT Image	Control Image	leonardo dicaprio wallpapers - wallpaper cave	Create wallpapers featuring a detailed black-and-white sketch of Leonardo DiCaprio, emphasizing his profile and in stylized line art or portrait.	The image shows Leonardo DiCaprio reclining on a luxurious white couch , dressed in ornate, gold- embroidered robes .	A stylish depiction of Leonardo DiCaprio seated in a casual pose indoors, with an backdrop featuring walls and furniture. He wears a loose-fitting shirt with long sleeves rolled up , captured in soft lighting with a gritty texture evoking cinematic artistry.

Figure 3: The enhanced prompts from different settings including zero shot model, model after SFT, and model after SFT and RFT.

This spatial information, together with the original text prompt, is employed to infer rich semantic elements that should appear in the target image, including objects and spatial relationships not explicitly mentioned in the original prompt but inferable from the control image. Meanwhile, to address the inherent limitations of control images (which may lack color and background information), we provide ground truth images to guide reasonable inferences about missing details. We denote our curated dataset as $D = \{(q^i, o^i)\}_{i=1}^N$, where q^i is the question for visual reasoning, and o^i is the response containing the chain-of-thought reasoning process and the resulting enhanced prompt P_{enh}^i .

We structure the outputs with a CoT reasoning process within `<think></think>` tags, followed by the resulting enhanced prompt enclosed in `<answer></answer>` tags. To ensure data quality, we filter out entries that do not conform to the required output format. It is worth noting that, to avoid trivial solutions derived directly from analyzing ground truth images, we exclude entries containing explicit references to these images. This curation process results in a small-scale but high-quality visual reasoning dataset tailored for the controllable image generation task.

3.2.2 Two-Phase Training

To fully harness the visual reasoning capabilities of MLLMs for control image interpretation, we implement a two-phase training strategy. The first phase involves supervised fine-tuning (SFT) on our curated small-scale visual reasoning dataset as a cold start to establish basic reasoning capabilities for control images. The second phase employs reinforcement fine-tuning (RFT) to evolve the model’s reasoning abilities through exploring different reasoning trajectories, guided by well-designed verifiable rewards.

Before implementing our two-phase chain-of-thought training strategy, we conducted preliminary experiments to examine the limitations of the zero-shot prompting MLLM. With zero-shot inference, the model consistently misinterpreted the high-contrast black-and-white stylistic implications of control images as an indication that the target image should adopt a line art aesthetic. As demonstrated in Fig. 3, the enhanced prompt of the zero-shot model incorrectly produced guidance for a line art composition rather than a realistic figure. Therefore, we first adopt SFT to address this problem.

SFT. Our first training phase employs supervised fine-tuning on the curated dataset to establish basic visual perception and reasoning capabilities. The supervised fine-tuning (SFT) objective can be expressed as:

$$\mathcal{L}_{SFT} = -\mathbb{E}_{(q,o) \sim D} [\log \pi_{\theta}(o|q)], \quad (2)$$

where π_{θ} is the policy model parameterized by θ .

As demonstrated in Fig. 3 While the model after SFT could interpret general style requirements, they frequently fabricated specific elements not supported by the control image, erroneously describing "luxurious white couch" when no such furniture was present in the control signal. This necessitate our second phase training strategy.

RFT. The second phase—reinforcement fine-tuning—is where the model’s reasoning abilities truly evolve. During this phase, for each question q , we generate multiple reasoning trajectories with diverse interpretations of the visual content. From each trajectory, we extract the final enhanced prompt $\{P_{enh}^1, P_{enh}^2, \dots, P_{enh}^N\}$ and evaluate its alignment with the ground truth image using CLIP scores as a verifiable reward metric. The reward for each enhanced prompt P_{enh}^i is calculated as:

$$R_{align} = \text{CLIP}(I_{gt}, P_{enh}^i), \quad (3)$$

where I_{gt} is the ground-truth image and CLIP computes the image-text similarity score.

Following DeepSeek-R1 [6], we introduce the format reward which verifies whether each response contains both the “<think></think>” and “<answer></answer>” tags, with the requirement that the “<think></think>” tags must precede the answer tags. Responses adhering to this format receive a reward of 1; otherwise, they receive 0. The final reward combines both the CLIP similarity score and this format adherence reward:

$$R(q, o^i) = R_{align} + R_{format} \quad (4)$$

This approach allows the model to learn from its own reasoning variations, identifying which reasoning pathways extract the most accurate and coherent dense semantic information. To systematically compare reasoning pathways, we implement Group Preference Optimization (GRPO), the relative advantage of each response within the group is computed as:

$$A_i = \frac{R_i - \text{mean}(\{R_1, \dots, R_G\})}{\text{std}(\{R_1, \dots, R_G\})}, \quad (5)$$

where $R_j = R(q, o^j)$ for $j = 1, 2, \dots, G$.

To maintain training stability and prevent excessive divergence from the reference model π_{ref} , we incorporate a KL divergence penalty weighted by coefficient β into our objective function. Finally, the objective function is calculated as:

$$\mathcal{L}_{\text{RFT}} = \mathbb{E}_{q \sim D} \left[\sum_{i=1}^G A_i \log \pi_{\theta}(o^i | q) - \beta \text{KL}[\pi_{\theta}(o^i | q) \parallel \pi_{\text{ref}}(o^i | q)] \right] \quad (6)$$

As evidenced in Fig. 3, our fully trained model demonstrates sophisticated understanding of implicit visual details from the control image ("casual pose indoor" and "long sleeves rolled up").

3.2.3 Inference Scaling

Due to the inherent limitations of control images, such as missing color information, background context, and other fine-grained details, the enhanced prompts, while semantically accurate, may still carry a degree of uncertainty. To mitigate this, we introduce an inference-time scaling strategy designed to fully leverage the model’s visual reasoning capabilities.

Specifically, we sample multiple enhanced prompts for the same control image and original text. Each enhanced prompt is used to generate a candidate image, which is then evaluated using our dual-metric assessment framework that accounts for both high-level semantic alignment and low-level visual fidelity. For high-level semantic evaluation, we adopt PickScore [12] to quantitatively assess the semantic alignment between each candidate image and the original prompt, as well as the overall fidelity of the candidate image. Simultaneously, for low-level layout evaluation, we calculate the LPIPS score [34] between the control map extracted from each candidate image and the original control image, quantifying structural fidelity. Formally, for a set of K candidate images $\{I_1, I_2, \dots, I_K\}$ generated from enhanced prompts $\{P_{enh}^1, P_{enh}^2, \dots, P_{enh}^K\}$ and the control image, we compute a combined reward score:

$$R(I_k) = \text{PickScore}(I_k, P_{orig}) - \text{LPIPS}(C(I_k), I_{control}) \quad (7)$$

where P_{orig} is the original prompt, $C(I_k)$ is the control map extracted from the generated image I_k , $I_{control}$ is the original control image. We select the candidate image with the highest reward:

$$I^* = \arg \max_{I_k} R(I_k) \quad (8)$$

This selected image excels in both fidelity, text alignment and structural adherence to the control signal.

4 Experiments

4.1 Experimental Setup

Datasets and Models. We implement our ControlThinker framework using Qwen2.5-VL-7B as the base MLLM for visual reasoning. For the data curation process, we leverage GPT-4o to generate

Table 1: **Conditional consistency of T2I controllable generation.** “↑” or “↓” indicate lower or higher values are better. “-” denotes that the method does not release a model for testing. The results are conducted on 512×512 resolution. “*” denotes that the performances are evaluated using the official open-source checkpoint, which is employed as our baseline.

Method	Seg	Canny	Hed	Lineart	Depth
	mIoU ↑	F1-Score ↑	SSIM ↑	SSIM ↑	RMSE ↓
	COCOStuff	MultiGen-20M	MultiGen-20M	MultiGen-20M	MultiGen-20M
GLIGEN [17]	-	26.94	-	-	38.83
T2I-Adapter [22]	-	23.65	-	-	48.40
Uni-ControlNet [35]	-	27.32	69.10	-	40.65
UniControl [24]	-	30.82	79.69	-	39.18
ControlNet [33]	27.46	34.65	76.21	70.54	35.90
ControlNet++ [15]	34.56	37.04	80.97	83.99	28.32
ControlAR* ² [18]	37.90	37.30	83.52	77.66	29.48
ControlThinker (Ours)	40.07	37.69	84.24	78.22	24.83

Table 2: **FID of T2I controllable generation.** “-” denotes that the method does not release a model for testing. Our ControlThinker achieves significant FID improvements. “*” shares the same meaning as in Tab. 1.

Method	Seg	Canny	Hed	Lineart	Depth
	COCOStuff	MultiGen-20M	MultiGen-20M	MultiGen-20M	MultiGen-20M
GLIGEN [17]	-	18.89	-	-	18.36
T2I-Adapter [22]	-	15.96	-	-	22.52
Uni-ControlNet [35]	-	17.14	17.08	-	20.27
UniControl [24]	-	19.94	15.99	-	18.66
ControlNet [33]	21.33	14.73	15.41	17.44	17.76
ControlNet++ [15]	19.29	18.23	15.01	13.88	16.66
ControlAR* [18]	14.31	24.08	12.52	14.39	17.38
ControlThinker (Ours)	14.09	19.76	11.39	12.68	16.07

high-quality reasoning outputs and enhanced prompts. Our controllable image generation experiments are conducted using ControlAR as the generator backbone, which is an autoregressive text-to-image model built on LlamaGen. We evaluate our approach across five control signal types: segmentation masks, canny edges, HED edges, lineart edges, and depth maps. For experiments on the segmentation mask, we utilize the COCOStuff dataset. For the four remaining control types, we employ the MultiGen-20M dataset, which contains various control signals paired with high-quality images and corresponding text prompts.

Implementation Details. For the data construction process, we generated approximately 6,000 high-quality CoT samples per control image category. For SFT, we adopt LoRA (rank=32, $\alpha=64$) with Adam optimizer (lr=5e-6, batch size=6) for one epoch. For RFT, we employed LoRA (rank=64, $\alpha=128$) with Adam (lr=1e-5, batch size=1), sampling 12 responses per question over 2,400 training steps. During inference scaling, we generated 10 enhanced prompts per data point, with each prompt generating one image and select the optimal one. All experiments are conducted on 8 NVIDIA A100 GPUs.

Evaluation Metrics. To assess controllable image generation capability, we adopt two metrics: conditional consistency and FID. Conditional consistency evaluates the structural fidelity between generated images and original control signals using task-specific metrics: mean Intersection-over-Union (mIoU) for segmentation masks, F1-Score for canny edges, Structural Similarity Index (SSIM) for HED and lineart edges, and Root Mean Square Error (RMSE) for depth maps. To evaluate overall generation quality, we utilize Fréchet Inception Distance (FID), which measures distributional similarity between generated and real images, with lower values indicating better image generation quality. Additionally, we employ PickScore to assess text-image alignment quality between generated prompts and real images.

²The open-source checkpoint is unified across multiple tasks, whereas the reported checkpoints in the paper were trained separately for each task.

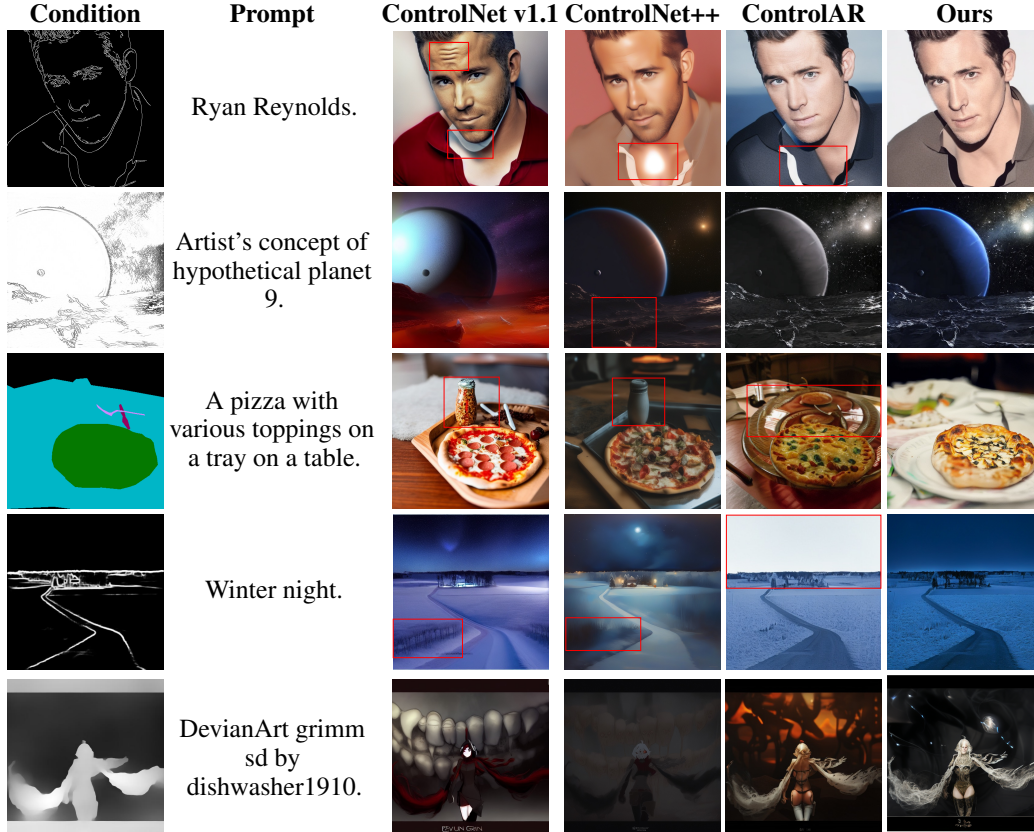


Figure 4: Qualitative comparison with prevalent approaches across different condition types.

4.2 Comparison with State-of-the-art Methods

Following the evaluation protocol of prior works [18, 15], we comprehensively compare our proposed method against ControlAR and other state-of-the-art baselines across two key dimensions: (1) structural fidelity to the control images, and (2) distributional realism with respect to ground-truth images. The results for each are presented in Tab. 1 and Tab. 2, respectively.

As shown in Tab. 1, our ControlThinker achieves state-of-the-art structural consistency across a range of conditional image generation tasks. Notably, it surpasses the well-trained ControlNet, its reinforcement learning enhanced counterpart ControlNet++, and the autoregressive baseline ControlAR* in preserving structural fidelity across Canny, HED, Seg, and Depth control conditions. Quantitatively, ControlThinker demonstrates significant gains, evidenced by a substantial increase of 2.17 in mIoU on the COCOStuff dataset for segmentation task and a notable reduction of 3.49 in RMSE on the MultiGen-20M dataset for depth task. These results underscore the superior capability of our proposed ControlThinker in generating images that exhibit both strong adherence to the input conditions and enhanced structural integrity compared to existing state-of-the-art methods.

Meanwhile, as demonstrated in Tab. 2, our ControlThinker also achieves state-of-the-art Fréchet Inception Distance (FID) scores across Seg, Hed, Lineart, and Depth tasks, indicating the superior image quality of our generated outputs. This consistent improvement in FID across various control conditions, achieved without fine-tuning the generator, highlights the efficacy of our method in providing higher-quality semantic information that enables the generator to produce better images while simultaneously maintaining structural integrity as shown in Tab. 1. The concurrent enhancement of both structural consistency and image quality underscores the effectiveness of ControlThinker in leveraging semantic guidance for improved image generation.

4.3 Comprehensive Analysis

Performances Breakdown. To systematically evaluate the effectiveness of each design in our proposed ControlThinker, we ablate their individual effects as shown in Tab. 4. We observe that

both SFT and the combination of SFT+RFT consistently improve SSIM and reduce FID across Hed and Lineart styles, indicating enhanced structural consistency and image quality. Besides, the addition of Inference Scaling further boosts SSIM but shows limited improvement in FID. It is worth noting that, our SFT+RFT configuration already surpasses Inference Scaling method in FID (11.78 vs. 12.17), suggesting that improving the reasoning module has a greater impact on image quality than sampling-based generation enhancements. Finally, our full ControlThinker model (i.e., combining SFT, RFT and Inference Scaling) achieves the best overall performance, confirming that reasoning improvements directly contribute to more faithful and higher-quality image generation.

Comparison between Enhanced and Original Prompts. To characterize our enhanced prompts following data curation, we analyze their length distribution compared to the original text prompts from the official dataset (Fig. 6). Our analysis reveals that the enhanced prompts are significantly longer than their original counterparts (note: lengths are calculated for final answers only, excluding Chain-of-Thought components). When combined with our use of ground-truth target images during curation (Sec. 3.2.1), these length-extended prompts demonstrate substantially richer semantic content. As we demonstrate in subsequent sections, this semantically enhanced dataset yields measurable improvements in model performance.

Table 3: Pickscore to evaluate image-text alignment. “Raw” represents the original text prompt in the official dataset.

Prompt Type	Hed	Lineart
Raw	20.23	20.23
SFT Gen.	20.33	20.49
SFT+RFT Gen.	20.37	20.68

Figure 5: Influences of different SFT approaches over RFT.

Method	Hed		Lineart	
	SSIM↑	FID↓	SSIM↑	FID↓
Baseline	83.52	12.52	77.66	14.39
+RFT	83.58	13.12	77.53	16.08
+SFT(w/o CoT)+RFT	<u>83.67</u>	<u>12.00</u>	<u>77.67</u>	<u>14.17</u>
+SFT(w/ CoT)+RFT	83.72	11.78	77.72	12.99

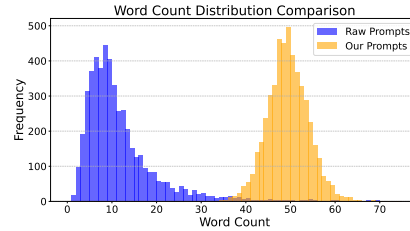
Evaluations of Generated Reasoning Responses. To further evaluate the reliability of the reasoning results of our ControlThinker, we further evaluate their alignment quality to the target image across the test set. As shown in Tab. 3, both SFT and the two-stage SFT+RFT training paradigms bring consistent improvements in Pickscore across Hed and Lineart styles compared to raw prompts. Specifically, the SFT-generated prompts already yield better alignment (20.33 for Hed and 20.49 for Lineart) than raw prompts (20.23 for both), indicating that supervised finetuning alone contributes positively to the alignment quality. Furthermore, applying RFT after SFT (SFT+RFT Gen.) achieves the best performance (20.37 for Hed and 20.68 for Lineart), demonstrating that RFT can further mine the reasoning potential of the model after SFT and refine the generation process. These results can act as intermediate metrics to verify the effectiveness of our proposed training paradigm in improving image-text alignment, a crucial factor for ultimate image generation.

Effects of SFT over RFT. Several contemporary studies [20, 21] have shown that applying domain-specific SFT prior to RFT can constrain the model’s search space, thereby limiting the potential benefits of RFT. In this part, we examine the effects of SFT over RFT in the controllable image generation task as shown in Fig. 5. Interestingly, applying RFT alone without prior SFT leads to degraded performance, with increased FID and slightly lower SSIM compared to the baseline. This suggests that the pre-trained MLLM’s initial understanding of the control image is insufficient, making the biased explorations during reinforcement learning. In contrast, introducing SFT with CoT-style reasoning data significantly improves performance, especially in FID (11.78 for Hed and 12.99

Table 4: Ablation study of each design in our method and their combination.

Method	Hed		Lineart	
	SSIM↑	FID↓	SSIM↑	FID↓
Baseline	83.52	12.52	77.66	14.39
+SFT	83.65	12.11	77.67	13.39
+SFT+RFT	83.72	<u>11.78</u>	<u>77.72</u>	<u>12.99</u>
+Inference Scaling	<u>84.02</u>	12.17	78.24	13.86
ControlThinker	84.24	11.39	<u>78.22</u>	12.68

Figure 6: Length distribution of text prompts in the official dataset versus our curated dataset enriched with visual semantics.



for Lineart), highlighting the importance of structured reasoning in interpreting the control image. The gap between using and omitting CoT during SFT confirms that control image understanding is a challenging task, and that explicit reasoning guidance during pretraining is crucial for enabling the model to generate higher-quality, semantically aligned outputs.

Qualitative Results Comparison. As shown in Fig. 4, our method generates results with higher visual fidelity and semantic accuracy. In the first row, other methods produce artifacts or distortions, while ours maintains facial realism. In the third row, ControlNet and ControlNet++ wrongly add condiment bottles, and ControlAR generates an extra tray. Only our model accurately follows both the layout and the prompt, demonstrating better structure understanding and semantic control.

5 Conclusion

In this paper, we present ControlThinker, a novel “comprehend-then-generate” framework that leverages a fine-tuned Multimodal Large Language Model (MLLM) to bridge the semantic gap in controllable image generation. By treating the MLLM as a visual reasoning engine, ControlThinker effectively extracts latent semantics from structurally sparse control images, enriching text prompts with denser guidance. Without modifying the image generator, our method achieves notable improvements in both visual fidelity and semantic alignment. Extensive experiments across multiple control types confirm the effectiveness of our approach.

References

- [1] Shuai Bai, Keqin Chen, Xuejing Liu, Jialin Wang, Wenbin Ge, Sibao Song, Kai Dang, Peng Wang, Shijie Wang, Jun Tang, Humen Zhong, Yanzhi Zhu, Mingkun Yang, Zhaohai Li, Jianqiang Wan, Pengfei Wang, Wei Ding, Zheren Fu, Yiheng Xu, Jiabo Ye, Xi Zhang, Tianbao Xie, Zesen Cheng, Hang Zhang, Zhibo Yang, Haiyang Xu, and Junyang Lin. Qwen2.5-vl technical report, 2025. URL <https://arxiv.org/abs/2502.13923>.
- [2] Xiaokang Chen, Zhiyu Wu, Xingchao Liu, Zizheng Pan, Wen Liu, Zhenda Xie, Xingkai Yu, and Chong Ruan. Janus-pro: Unified multimodal understanding and generation with data and model scaling. *arXiv preprint arXiv:2501.17811*, 2025.
- [3] Huilin Deng, Ding Zou, Rui Ma, Hongchen Luo, Yang Cao, and Yu Kang. Boosting the generalization and reasoning of vision language models with curriculum reinforcement learning. *arXiv preprint arXiv:2503.07065*, 2025.
- [4] Prafulla Dhariwal and Alexander Nichol. Diffusion models beat gans on image synthesis. *Advances in neural information processing systems*, 34:8780–8794, 2021.
- [5] Rongyao Fang, Chengqi Duan, Kun Wang, Linjiang Huang, Hao Li, Shilin Yan, Hao Tian, Xingyu Zeng, Rui Zhao, Jifeng Dai, et al. Got: Unleashing reasoning capability of multimodal large language model for visual generation and editing. *arXiv preprint arXiv:2503.10639*, 2025.
- [6] Daya Guo, Dejian Yang, Haowei Zhang, Junxiao Song, Ruoyu Zhang, Runxin Xu, Qihao Zhu, Shirong Ma, Peiyi Wang, Xiao Bi, et al. Deepseek-r1: Incentivizing reasoning capability in llms via reinforcement learning. *arXiv preprint arXiv:2501.12948*, 2025.
- [7] Ziyu Guo, Renrui Zhang, Chengzhuo Tong, Zhizheng Zhao, Peng Gao, Hongsheng Li, and Pheng-Ann Heng. Can we generate images with cot? let’s verify and reinforce image generation step by step. *arXiv preprint arXiv:2501.13926*, 2025.
- [8] Jonathan Ho, Ajay Jain, and Pieter Abbeel. Denoising diffusion probabilistic models. *Advances in neural information processing systems*, 33:6840–6851, 2020.
- [9] Minghui Hu, Jianbin Zheng, Daqing Liu, Chuanxia Zheng, Chaoyue Wang, Dacheng Tao, and Tat-Jen Cham. Cocktail: Mixing multi-modality control for text-conditional image generation. In *Thirty-seventh Conference on Neural Information Processing Systems*, 2023.
- [10] Shanshan Huang, Qingsong Li, Jun Liao, Shu Wang, Li Liu, and Lian Li. Controllable image synthesis methods, applications and challenges: a comprehensive survey. *Artificial Intelligence Review*, 57(12):336, 2024.

- [11] Yang Jiao, Haibo Qiu, Zequn Jie, Shaoxiang Chen, Jingjing Chen, Lin Ma, and Yu-Gang Jiang. Unitoken: Harmonizing multimodal understanding and generation through unified visual encoding. *arXiv preprint arXiv:2504.04423*, 2025.
- [12] Yuval Kirstain, Adam Polyak, Uriel Singer, Shahbuland Matiana, Joe Penna, and Omer Levy. Pick-a-pic: An open dataset of user preferences for text-to-image generation. *Advances in Neural Information Processing Systems*, 36:36652–36663, 2023.
- [13] Black Forest Labs. Flux. <https://github.com/black-forest-labs/flux>, 2024.
- [14] Bo Li, Yuanhan Zhang, Dong Guo, Renrui Zhang, Feng Li, Hao Zhang, Kaichen Zhang, Peiyuan Zhang, Yanwei Li, Ziwei Liu, et al. Llava-onevision: Easy visual task transfer. *arXiv preprint arXiv:2408.03326*, 2024.
- [15] Ming Li, Taojiannan Yang, Huafeng Kuang, Jie Wu, Zhaoning Wang, Xuefeng Xiao, and Chen Chen. Controlnet++: Improving conditional controls with efficient consistency feedback: Project page: liming-ai. [github.io/controlnet_plus_plus](https://github.com/liming-ai/controlnet_plus_plus). In *European Conference on Computer Vision*, pages 129–147. Springer, 2024.
- [16] Xiang Li, Kai Qiu, Hao Chen, Jason Kuen, Zhe Lin, Rita Singh, and Bhiksha Raj. Controlvar: Exploring controllable visual autoregressive modeling. *arXiv preprint arXiv:2406.09750*, 2024.
- [17] Yuheng Li, Haotian Liu, Qingyang Wu, Fangzhou Mu, Jianwei Yang, Jianfeng Gao, Chunyuan Li, and Yong Jae Lee. Gligen: Open-set grounded text-to-image generation. In *Proceedings of the IEEE/CVF conference on computer vision and pattern recognition*, pages 22511–22521, 2023.
- [18] Zongming Li, Tianheng Cheng, Shoufa Chen, Peize Sun, Haocheng Shen, Longjin Ran, Xiaoxin Chen, Wenyu Liu, and Xinggang Wang. Controlar: Controllable image generation with autoregressive models. *arXiv preprint arXiv:2410.02705*, 2024.
- [19] Jiaqi Liao, Zhengyuan Yang, Linjie Li, Dianqi Li, Kevin Lin, Yu Cheng, and Lijuan Wang. Imagegen-cot: Enhancing text-to-image in-context learning with chain-of-thought reasoning. *arXiv preprint arXiv:2503.19312*, 2025.
- [20] Ziyu Liu, Zeyi Sun, Yuhang Zang, Xiaoyi Dong, Yuhang Cao, Haodong Duan, Dahua Lin, and Jiaqi Wang. Visual-rft: Visual reinforcement fine-tuning. *arXiv preprint arXiv:2503.01785*, 2025.
- [21] Fanqing Meng, Lingxiao Du, Zongkai Liu, Zhixiang Zhou, Quanfeng Lu, Daocheng Fu, Tiancheng Han, Botian Shi, Wenhai Wang, Junjun He, et al. Mm-eureka: Exploring the frontiers of multimodal reasoning with rule-based reinforcement learning. *arXiv preprint arXiv:2503.07365*, 2025.
- [22] Chong Mou, Xintao Wang, Liangbin Xie, Yanze Wu, Jian Zhang, Zhongang Qi, and Ying Shan. T2i-adapter: Learning adapters to dig out more controllable ability for text-to-image diffusion models. In *Proceedings of the AAAI conference on artificial intelligence*, volume 38, pages 4296–4304, 2024.
- [23] William Peebles and Saining Xie. Scalable diffusion models with transformers. In *Proceedings of the IEEE/CVF international conference on computer vision*, pages 4195–4205, 2023.
- [24] Can Qin, Shu Zhang, Ning Yu, Yihao Feng, Xinyi Yang, Yingbo Zhou, Huan Wang, Juan Carlos Niebles, Caiming Xiong, Silvio Savarese, et al. Unicontrol: A unified diffusion model for controllable visual generation in the wild. *arXiv preprint arXiv:2305.11147*, 2023.
- [25] Robin Rombach, Andreas Blattmann, Dominik Lorenz, Patrick Esser, and Björn Ommer. High-resolution image synthesis with latent diffusion models. In *Proceedings of the IEEE/CVF conference on computer vision and pattern recognition*, pages 10684–10695, 2022.
- [26] Haozhan Shen, Peng Liu, Jingcheng Li, Chunxin Fang, Yibo Ma, Jiajia Liao, Qiaoli Shen, Zilun Zhang, Kangjia Zhao, Qianqian Zhang, et al. Vlm-r1: A stable and generalizable r1-style large vision-language model. *arXiv preprint arXiv:2504.07615*, 2025.

- [27] Fangxun Shu, Yue Liao, Le Zhuo, Chenning Xu, Lei Zhang, Guanghao Zhang, Haonan Shi, Long Chen, Tao Zhong, Wanggui He, et al. Llava-mod: Making llava tiny via moe knowledge distillation. *arXiv preprint arXiv:2408.15881*, 2024.
- [28] Peize Sun, Yi Jiang, Shoufa Chen, Shilong Zhang, Bingyue Peng, Ping Luo, and Zehuan Yuan. Autoregressive model beats diffusion: Llama for scalable image generation. *arXiv preprint arXiv:2406.06525*, 2024.
- [29] Yanan Sun, Yanchen Liu, Yinhao Tang, Wenjie Pei, and Kai Chen. Anycontrol: create your artwork with versatile control on text-to-image generation. In *European Conference on Computer Vision*, pages 92–109. Springer, 2024.
- [30] Xudong Wang, Trevor Darrell, Sai Saketh Rambhatla, Rohit Girdhar, and Ishan Misra. Instancediffusion: Instance-level control for image generation. In *Proceedings of the IEEE/CVF Conference on Computer Vision and Pattern Recognition*, pages 6232–6242, 2024.
- [31] Yi Yang, Xiaoxuan He, Hongkun Pan, Xiyan Jiang, Yan Deng, Xingtao Yang, Haoyu Lu, Dacheng Yin, Fengyun Rao, Minfeng Zhu, et al. R1-onevision: Advancing generalized multimodal reasoning through cross-modal formalization. *arXiv preprint arXiv:2503.10615*, 2025.
- [32] Jingyi Zhang, Jiaxing Huang, Huanjin Yao, Shunyu Liu, Xikun Zhang, Shijian Lu, and Dacheng Tao. R1-vl: Learning to reason with multimodal large language models via step-wise group relative policy optimization. *arXiv preprint arXiv:2503.12937*, 2025.
- [33] Lymin Zhang, Anyi Rao, and Maneesh Agrawala. Adding conditional control to text-to-image diffusion models. In *Proceedings of the IEEE/CVF international conference on computer vision*, pages 3836–3847, 2023.
- [34] Richard Zhang, Phillip Isola, Alexei A Efros, Eli Shechtman, and Oliver Wang. The unreasonable effectiveness of deep features as a perceptual metric. In *Proceedings of the IEEE conference on computer vision and pattern recognition*, pages 586–595, 2018.
- [35] Shihao Zhao, Dongdong Chen, Yen-Chun Chen, Jianmin Bao, Shaozhe Hao, Lu Yuan, and Kwan-Yee K Wong. Uni-controlnet: All-in-one control to text-to-image diffusion models. *Advances in Neural Information Processing Systems*, 36:11127–11150, 2023.
- [36] Dewei Zhou, You Li, Fan Ma, Xiaoting Zhang, and Yi Yang. Migc: Multi-instance generation controller for text-to-image synthesis. In *Proceedings of the IEEE/CVF Conference on Computer Vision and Pattern Recognition*, pages 6818–6828, 2024.